Ultrafast pulse characterization using XPM in silicon

Nuh S. Yuksek, Xinzhu Sang, En-Kuang Tien, Qi Song, Feng Qian, Ivan V. Tomov, Ozdal Boyraz
Department of Electrical Engineering & Computer Science, University of California, Irvine, Irvine, CA, USA 92697

ABSTRACT

Due to the high-index contrast between the silicon core and silica cladding, the silicon waveguide allows strong optical confinement and large effective nonlinearity, which facilitates low cost chip scale demonstration of all-optical nonlinear functional devices at relatively low pump powers. One of the challenges in ultrafast science is the full characterization of optical pulses in real time. The time-wavelength mapping is proven to be a powerful technique for real time characterization of fast analog signals. Here we demonstrated a technique based on the cross-phase modulation (XPM) between the short pulse and the chirped supercontinuum (SC) pulse in the silicon chip to map fast varying optical signals into spectral domain. In the experiment, when 30 nm linearly chirped supercontinuum pulses generated in a 5 km dispersion-shifted fiber at the normal regime and 2.4 ps pulse are launched into a 1.7 cm silicon chip with 5 μm^2 modal area, a time-wavelength mapped pattern of the short pulses is observed on the optical spectrum analyzer. From the measured spectral mapping the actual 2.4ps temporal pulse profile is reconstructed in a computer. This phenomenon can be extended to full characterization of amplitude and phase information of short pulses. Due to time wavelength mapping this approach can also be used in real time amplitude and phase measurement of ultrafast optical signals with arbitrary temporal width. The high nonlinearity and negligible distortions due to walk off make silicon an ideal candidate for XPM based measurements.

Keywords: Pulse measurement, frequency resolved optical gating.

1. INTRODUCTION

The progress in the development of ultrafast lasers has driven the requirement of the detail characteristic of an ultrafast pulse[1]. Frequency-resolved optical gating (FROG) and autocorrelation measurement [2,3] techniques have been well developed for measuring and characterizing the ultrafast pulses. FROG technique has advantages over the autocorrelator because it can measure detailed pulse shape instead of assuming Gaussian pulse shape in autocorrelators, and it can provide phase information. Both the techniques are applying optical nonlinear properties in the measurement. Silicon photonics has attracted a lot of attention because of its advances in nonlinear properties. The major two advantages of silicon nonlinear optics are: strong optical confinement due to large refractive index difference between silicon core and glass cladding, and large Raman and Kerr nonlinearities which are about 1000 and 200 times higher than those of silica. The combination leads to efficient optical nonlinear phenomena and devices which have been demonstrated at relative low power levels. For example, Raman lasing and amplification [4,5], self-phase modulation (SPM) and cross-phase modulation(XPM)[6, 7], parametric generation and amplifier [8], four-wave fixing wavelength conversion [9-12] and a time lens [13] have been demonstrated. Therefore, silicon is an ideal material for miniaturized nonlinear optical devices and instruments. In this paper, we present study of the cross-phase modulation (XPM) in silicon for ultrafast pulse

Photonic Fiber and Crystal Devices: Advances in Materials and Innovations in Device Applications II, edited by Shizhuo Yin, Ruyan Guo,
Proc. of SPIE Vol. 7056, 705611, (2008) · 0277-786X/08/$18 · doi: 10.1117/12.795606

measurement and application. We also show that the XPM between the two pulses induces spectral change which can be mapped to the time domain by inserting linearly chirp after the XPM process and can be processed in real time.

2. PULSE CHARACTERIZATION BY XPM AND TIME - WAVELENGTH MAPPING

2.1 Principle

Conventional FROG analysis utilizes spectral scanning or time averaged scanning of two identical pulses. Having real time pulse scan can provide information that can never be attained by the conventional approach. Time wavelength mapping with XMP FROG analysis can provide this real time information provided that we have highly nonlinear medium with negligible walk-off. Due to high modal confinement in silicon waveguide, the nonlinear effects become more efficient. Even at low power levels of the pulses can generate nonlinear phase shift in time domain which translates into XPM induced modulation pattern. For instance, Figure1 illustrates the nonlinear interaction between a short pulse laser and a chirped broadband optical signal, a supercontinuum (SC) source. The XPM process induces modulation pattern in frequency domain which can be transformed into time domain by known dispersive element such as a grating. Since the SC is linearly chirped i.e. it has a time to wavelength mapping, the time delay between SC pulse peak position and probe pulse will also be visible in spectral domain. Assuming that the SC and probe source are orthogonally polarized, the supercontinuum after XPM in the silicon-on-insular (SOI) waveguide can be express as:

$$E_{SC}(z,t) = E_{SC}(0,t-\sigma z)\cdot\exp\left[i\gamma\left|E_{SC}(0,t-\sigma z)\right|^2 + \frac{2}{3}i\gamma\left|\int_{-L}^{L} E_{probe}(0,t-\tau+\sigma\zeta)\,d\zeta\right|^2\right] \quad (1)$$

Where E_{sc}, E_{probe} is the electric field if the supercontinuum and probe pulse. σ is the birefringence coefficient, γ is the Kerr nonliearn coefficient and L is the waveguide length.

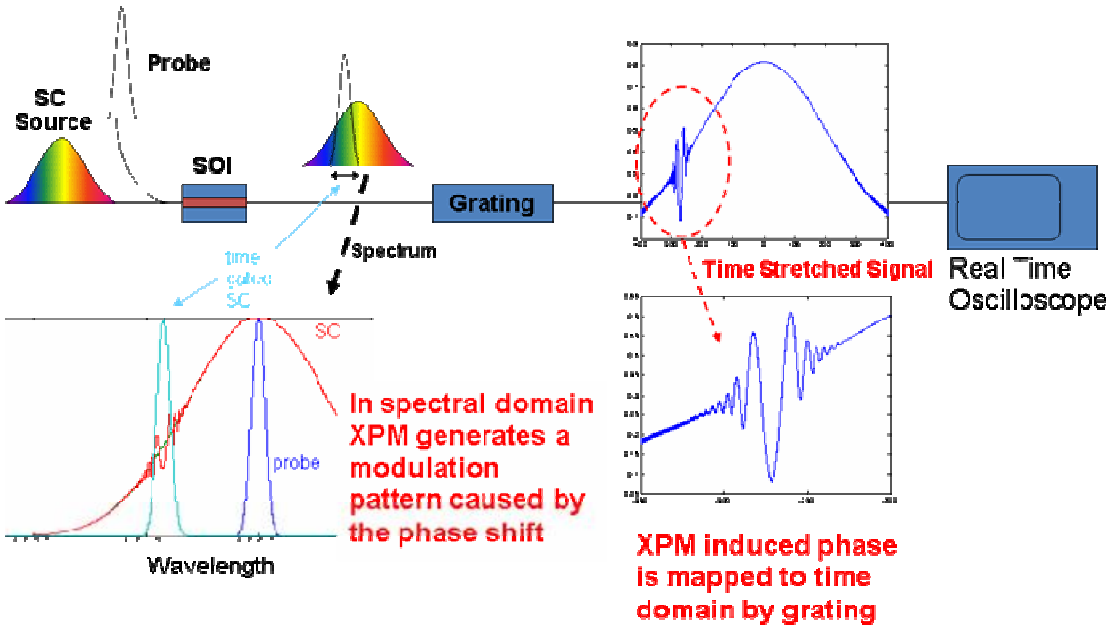

Fig. 1 Principle of the pulse characterize using XPM based time - wavelength mapping

By comparing the original spectrum and the spectrum measured after the XPM process we can extract information regarding the phase and amplitude information of a chirped broadband source for a known pump intensity profile. For example, if we assume a Gaussian probe with no phase information and a linearly chirped SC, the XPM in equation (1) will create a modulation in a time domain and result in a Gaussian modulation pattern generated on top of the SC spectrum, as depicted in Figure 2.

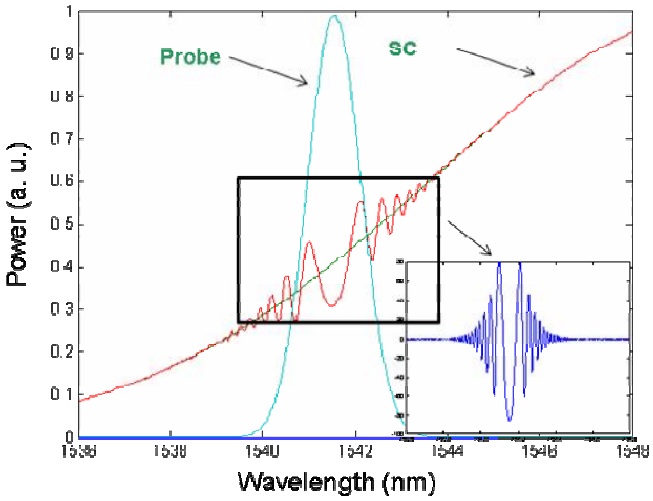

Fig. 2 Modulation pattern created by XPM at wavelength domain. Inlet: Normalized pattern.

The width and amplitude of the modulation envelope are defined by the probe width and intensity. The period of the modulation pattern is defined by the chirp characteristics of the SC pulse. Spectral position of the modulation pattern is also defined by the time delay between the probe and chirp of the continuum pulse, Figure 3.

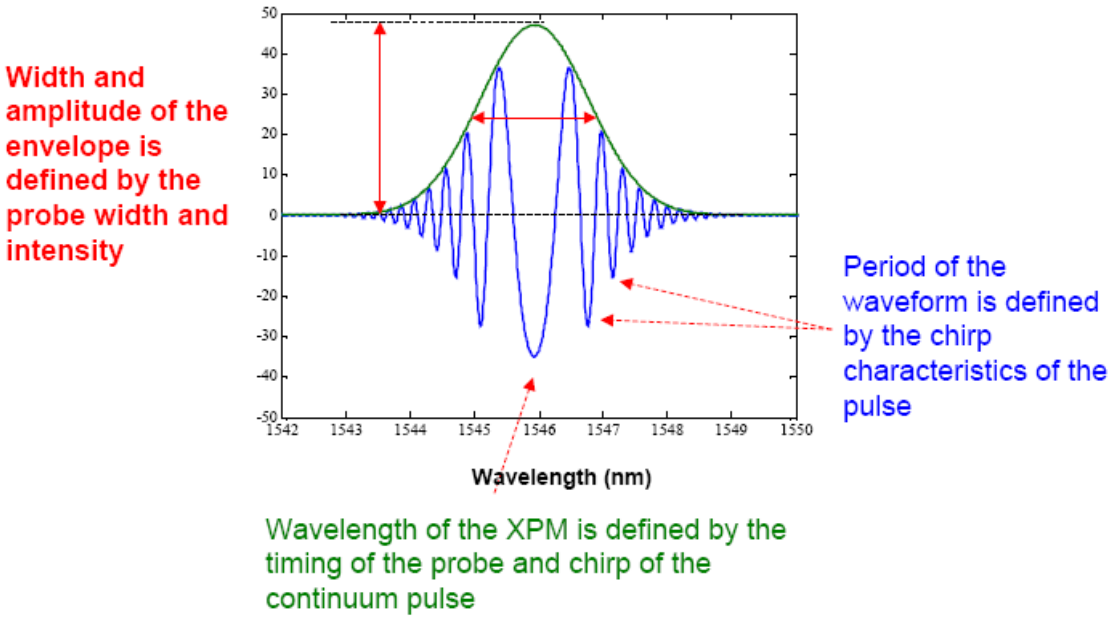

Fig.3 Time-wavelength maping of the pulse characteristics

Figure 4 shows the SC chirp dependence of the XPM spectrum. Larger chirp of the SC causes increase of frequency of the fluctuations in the frequency domain and does not change the profile of the XPM. This property enables us to analyze the chirp characteristic of a SC with this method.

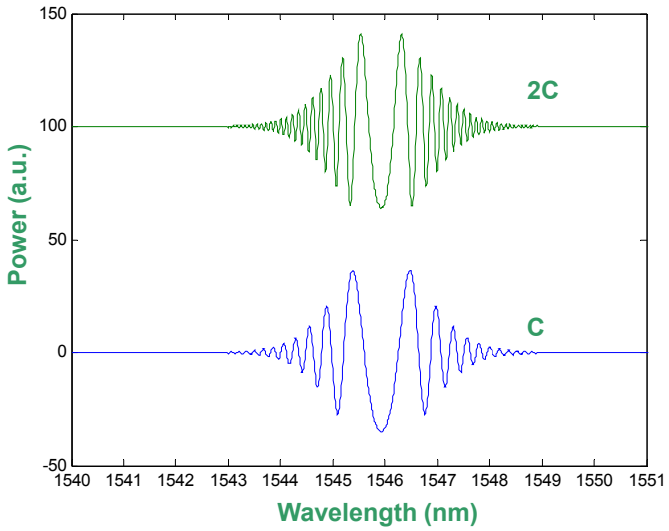

Fig. 4 XPM pattern at frequency domain of two difference chirped SC and the probe pulse.

2.2 EXPERIMENTAL RESULTS

The experimental setup of ultrafast pulse characterization by XPM in silicon is demonstrated by a linearly chirped SC source, a short pulse laser source and a SOI waveguide as shown in Fig.5. Linearly chirped SC source was obtained by propagate a modelocked laser pulse in a 5 km dispersion-shifted-fiber with at normal dispersion regime (D= -2 ps/nm·km). The probe pulse is generated using the same modelocked laser; connected to a 1.6nm optical band pass filter and an EDFA. Two pulses are combined by a WDM coupler before entering the 1.7 cm Silicon-on-Insulator (SOI) waveguide with ~5μm^2 modal area. The output signal is detected by an optical spectrum analyzer and the data was processed using a PC.

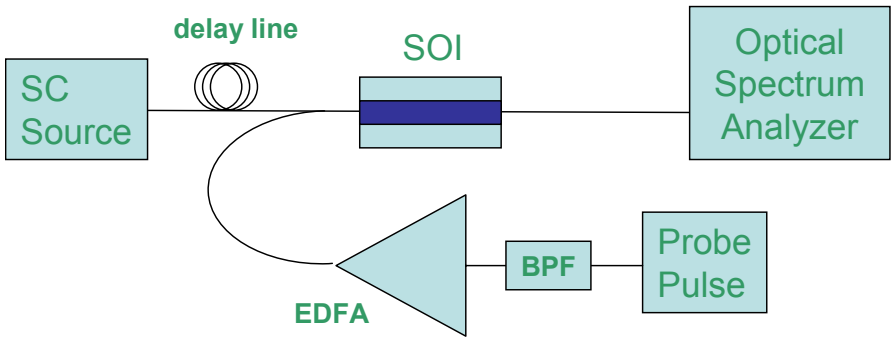

Fig. 5 Experimental setup for an ultrafast pulse characterization by XPM in Si

Figure 6 shows the XPM of the SC with different probe power values. The amplitude of the modulation in the frequency domain changes with the probe intensity. For constant pump power and pulse width, the width of the modulation pattern remains the same. By using a simple signal processing algorithm fed by the modulation pattern, the

pump pulse width is obtained to be 2.4ps. As expected, based on the time delay between SC and probe pulses, up to 30% amplitude modulation of the SC at a certain wavelength is observed due to XPM. The difference between SC and cross phase modulated spectra is carrying the information about the SC chirp properties and probe pulse amplitude characteristics. Further analysis can be carried out to fully characterize the chirped SC source.

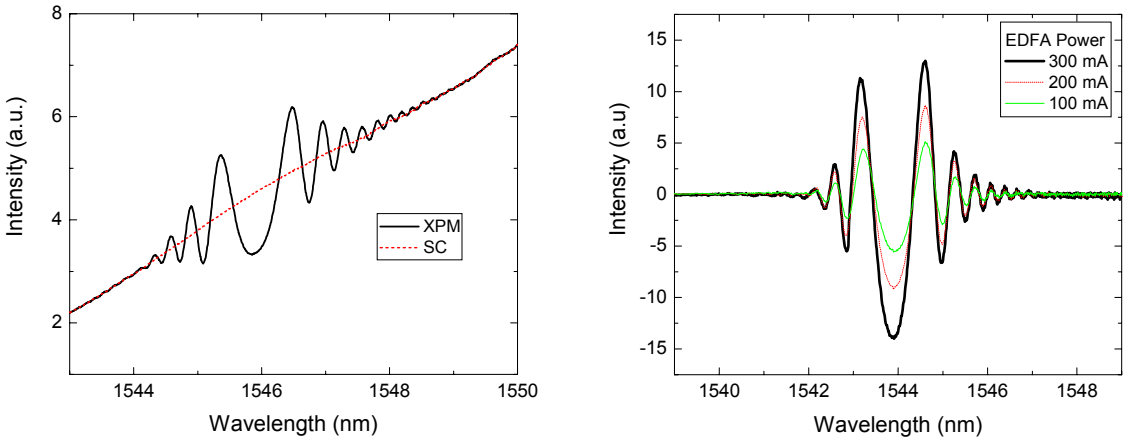

Fig. 6 (a) Modulation pattern measured on OSA and (b) Normalized modulation pattern with different probe power.

3. CROSS-PHASE-MODULATION FROG BASED ON SILICON

A well established second harmonics generation (SHG) FROG is a powerful tool to measure ultrafast pulses with a few femtoseconds pulse width. Other than SHG, there are different types of FROG, such as polarization gate FROG, self-diffraction FROG, third harmonic generation FROG and XPM FROG [1-3]. XPM FROG was proposed and has been demonstrated by using bulk silica [14], single mode fiber [15], microstructure optical fiber [16], and a quantum well structure device [17] as the nonlinear medium. The advantage of using XPM FROG is that, SHG FROG has an ambiguity in the direction of time of the retrieved pulse and XPM FROG can provide a comparable sensitivity without ambiguity. Here we show that high nonlinearity and negligible walk-off provided by silicon waveguides can be ideal for FROG measurements.

The experimental setup of silicon XPM FROG is shown in Figure 7. The incident pulses are separated by a polarization beam coupler/splitter (PBC) into two polarization components that are orthogonal to each other. The ratio between two branches can be controlled by the polarization controller at the input. An optical delay line constructed by two fiber collimators and a moving stage is used to produce time delay between two polarizations. After passing the delay line, the two polarization are combined by another PBC and entering a 1.7cm SOI waveguide. The waveguide has 5 μm^2 modal area. Probe pulse is selected by a PBS at the output of the waveguide. We use an optical spectrum analyzer (OSA) to measure the spectrum and generate the spectrogram. The probe signal selected at the output of the PBS can be written as [16]:

$$E_{sig}(t,\tau) = E_p(t)\exp\left[\frac{2}{3}i\gamma\left|E_G(t-\tau)\right|^2\right] \tag{2}$$

Where $E_p(t)$, $E_G(t)$ is the field in the two polarization branches. Here we assume $E_p(t)$ is much smaller than $E_G(t)$ and thus the self phase modulation can be ignored. The FROG signal measured by the spectrum analyzer is:

$$I(\omega,\tau)=\left|\int_{-\infty}^{\infty}E_{sig}(t,\tau)e^{i\omega t}dt\right|^2 \tag{3}$$

The spectrogram is generated by measuring spectrum with different delay τ between two signals. The pulse amplitude and phase information then can be retrieved from the spectrogram by using principal component generalized projections (PCGP) algorithm [18]. In the PCGP algorithm some criteria of the probe and gate is required to avoid ambiguous solutions. For example, in SHG FROG the criteria is Pt=Gt. Here we treat the probe field E_P as the input P_t and the XPM exponential term $\exp(2/3i\gamma|E_G(t-\tau)|^2)$ in (2) as the gate function G_t. Since the gate is only a phase modulation the amplitude of G_t is reset to one in each itineration while keep the phase information.

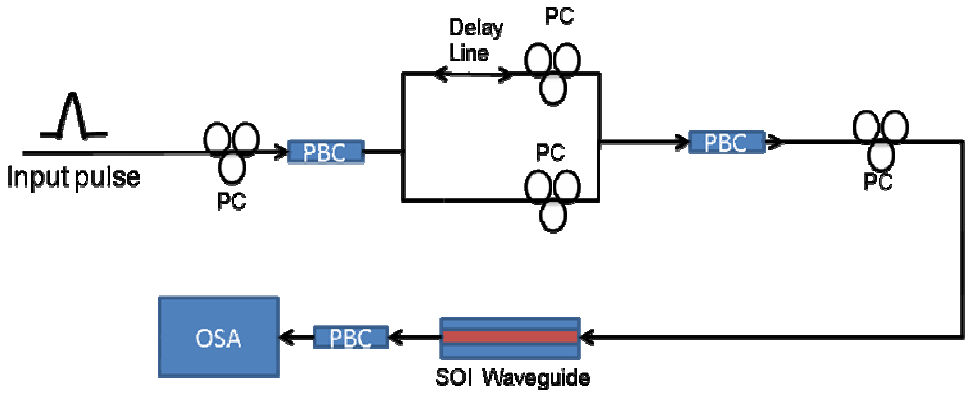

Fig. 7 Experimental setup of XPM FROG. PC: polarization controller; PBC: polarization beam coupler; OSA: optical spectrum analyzer.

The experimental result for measuring a femtosecond modelocked fiber laser is shown in Figure 8. The spectrogram is taken within 12.8 ps time delay. The retrieved pulse and the phase are shown in Figure 9. It reveals that the input pulse has a pulse width ~700fs, which matches the spec of the modelocked laser. The error is 4.5% which is mainly due to noise in the spectrum analyzer. As illustrated in the previous section, the time wavelength mapping can be adapted here for real time characterization of femtosecond optical pulses.

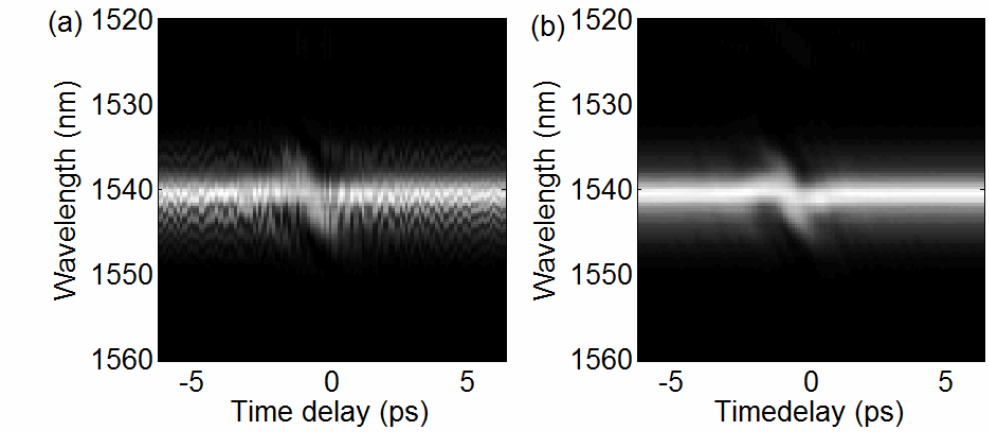

Fig. 8 (a)Measured and (b) retrieved FROG traces

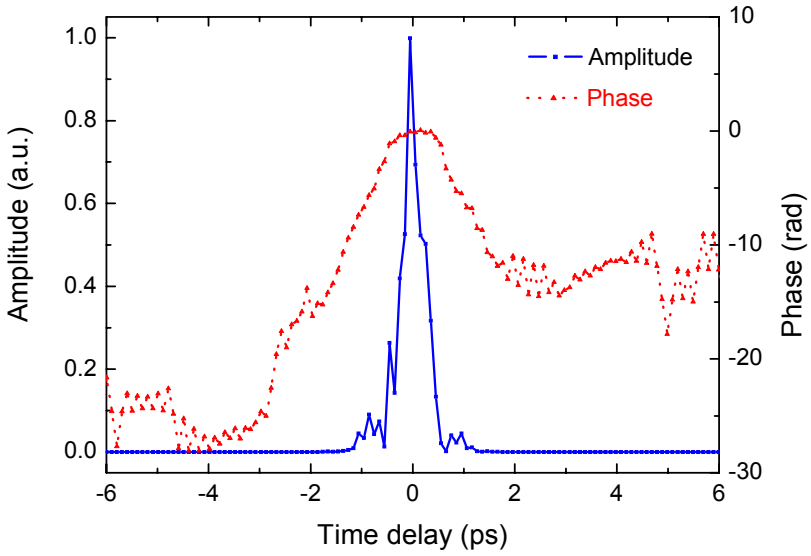

Fig. 9 Retrieved pulse and phase.

4. CONCLUSION

A novel approach for measuring ultrafast pulse using cross-phase-modulation in silicon has been proposed and demonstrated. With the time-frequency mapping the XPM can be used as a pulse measurement tool with single shot spectrum measurement and a simple fitting. The concept can be extended to XPM FROG measurement in silicon. The measured result using XPM FROG based on silicon is presented.

This work supported by DARPA under SSC San Diego grant No. N66001-07-1-2007.

REFERENCE

[1] C. Dorrer, and I. A. Walmsley, “Concepts for the Temporal Characterization of Short Optical Pulses,” EURASIP Journal on Advances in Signal Processing, 2005(10), 1541 (2005).
[2] J. Paye, “How to measure the amplitude and phase of an ultrashort light pulse with an autocorrelator and a spectrometer,” Quantum Electronics, IEEE Journal of, 30(11), 2693 (1994).
[3] R. Trebino, [Frequency-Resolved Optical Gating: The Measurement of Ultrashort Laser Pulses] Springer, (2002).
[4] O. Boyraz and B. Jalali, “A Demonstration of a silicon Raman laser,” Optics Express, 12(21), 5269 (2004).
[5] X. Sang, E.-K.Tien, N. S. Yuksek, F. Qian, Q. Song, O. Boyraz, "Dual-wavelength mode-locked fiber laser with an intracavity silicon waveguide," IEEE Photon. Techno. Lett., 20(13),1184(2008).
[6] E. Dulkeith, Y. A. Vlasov, X. Chen et al., “Self-phase-modulation in submicron silicon-on-insulator photonic wires,” Opt. Express, 14(12), 5524 (2006).
[7] O. Boyraz, P. Koonath, V. Raghunathan et al., “All optical switching and continuum generation in silicon waveguides,” Optics Express, 12(17), 4094 (2004).
[8] M. A. Foster, A. C. Turner, J. E. Sharping et al., “Broad-band optical parametric gain on a silicon photonic chip,” Nature, 441(7096), 960-963 (2006).

[9] H. Fukuda, K. Yamada, T. Shoji et al., "Four-wave mixing in silicon wire waveguides," Opt. Express, 13(12), 4629 (2005).
[10] H. Rong, Y.-H. Kuo, A. Liu et al., "High efficiency wavelength conversion of 10 Gb/s data in silicon waveguides," Opt. Express, 14(3), 1182 (2006).
[11] R. Espinola, J. Dadap, J. R. Osgood et al., "C-band wavelength conversion in silicon photonic wire waveguides," Opt. Express, 13(11), 4341 (2005).
[12] A. C. Turner, M. A. Foster, A. L. Gaeta et al., "Ultra-low power parametric frequency conversion in a silicon microring resonator," Opt. Express, 16(7), 4881 (2008).
[13] R. Salem, M. A. Foster, A. C. Turner et al., "Optical time lens based on four-wave mixing on a silicon chip," Opt. Lett., 33(10), 1047 (2008).
[14] H. R. Lange, M. A. Franco, J. F. Ripoche et al., "Reconstruction of the time profile of femtosecond laser pulses through cross-phase modulation," IEEE Journal of Selected Topics in Quantum Electronics, 4(2), 295-300 (1998).
[15] M. D. Thomson, J. M. Dudley, L. P. Barry et al., "Complete pulse characterization at 1.5μ m by cross-phase modulation in optical fibers," Opt. Lett., 23(20), 1582 (1998).
[16] P. Honzatko, J. Kanka, and B. Vrany, "Measurement of pulse amplitude and phase using cross-phase modulation in microstructure fiber," Optics Letters, 30(14), 1821-1823 (2005).
[17] D. Reid, P. J. Maguire, L. P. Barry et al., "All-optical sampling and spectrographic pulse measurement using cross-absorption modulation in multiple-quantum-well devices," J. Opt. Soc. Am. B, 25(6), A133 (2008).
[18] D. J. Kane, "Real-time measurement of ultrashort laser pulses using principal component generalized projections," Selected Topics in Quantum Electronics, IEEE Journal of, 4(2), 278 (1998).